Chemical Papers (2020) 74:4213–4226
https://doi.org/10.1007/s11696-020-01236-9

ORIGINAL PAPER

Schiff base of 4*E*,10*E*-4-(2-(4-nitrophenyl)-*N*-((1H-indol-3-yl) methylene) benzenamine-based "turn-on" fluorescence chemosensor for highly selective detection of Ni^{2+}, Fe^{3+}, and Mg^{2+} ions

Mathivanan Iyappan[1] · Ezhumalai Dhineshkumar[1] · Chinnadurai Anbuselvan[1,2]

Received: 4 April 2020 / Accepted: 29 May 2020 / Published online: 7 June 2020

Abstract

A Schiff base of 4*E*,10*E*-4-(2-(4-nitrophenyl)-*N*-((1H-indol-3-yl)methylene) benzenamine was synthesized and characterized by $^{1}H\&^{13}C$-NMR, FT-IR, and ESI–MS spectroscopy. UV–visible and fluorescence studies were explored for chemosensor **ICPA** to detect Ni^{2+}, Fe^{3+}, and Mg^{2+} by fluorescence chemosensor "turn-on" method in 10 mM HEPES buffer in EtOH/H_2O (1:4, *v*/*v*) medium. Chemosensor **ICPA** binds with the selective heavy metal ions and could be proved in very low detection limits. Job's plot demonstrates 1:1 stoichiometric complexes of **ICPA** + Ni^{2+}, **ICPA** + Fe^{3+}, and **ICPA** + Fe^{3+} with the calculated mole fraction of 0.5 µM. Binding constant values calculated using the Benesi–Hildebrand method are found to be 3.45×10^{8} M^{-2}, 5.63×10^{4} M^{-2}, and 8.63×10^{3} M^{-2}, respectively. Competitive metal ions tests were also carried out with transition metal ions. Furthermore, HeLa cell activity at different concentrations added with ligand to perform inhibition capability of the probe was also carried out.

Keywords Synthesis · Fluorescent · Chemosensor · Nickel, iron, and magnesium · HeLa cells

Introduction

Fluorescent chemosensors attracted a huge deal of interest due to their high simplicity, sensitivity, versatility, selectivity, and capabilities through the sensing of various chemical, biological, and environmental significance species, including metal ions and anions, between in vitro and also in vivo (Yiran et al. 2014), and, in addition, portability and the availability of a broad variety as indicator dyes. There is nothing to doubt fluorescent chemosensors with their different responsibilities against several analytes for cost-effective and instrumental practical applications (Sun et al. 2017). In earlier studies, small molecular-structured fluorescent chemosensors are used as a monitoring agent over the analyte in a living system. These contained high selectivity and sensitivity with uncomplicated recognition procedures. Therefore, this decade has seen various experiments paying attention to the construction of sensitive and selective chemosensors using spectral techniques with both spectrofluorometric and spectrophotometric techniques for the recognition (Vijay et al. 2019). In general, chemosensors either enhance or reduce the emission and absorption band due to binding with metal ions (Nayab and Shkir 2017). The most benefit of fluorescence "turn-on" chemosensors related to "turn-off" chemosensors is for their low concentration compared to a "dark" background, which decreases the opportunity of wrong positive signals and enhances the sensitivity, as established by several studies. Moreover, colorimetric chemosensors got involved in much attention for allowed "naked-eye" recognition in a difficult and inexpensive method, to contribute qualitative and quantitative information (Li et al. 2014). Detection and sense of different metal ions have to befall a dynamic field of analysis due to its potential application in various fields including such as biomedicine, chemistry, and finally environmental studies (Hyvönen and Aksela 2010). The high content of transition and heavy metals in soil, air, drinking water, and plants is

Electronic supplementary material The online version of this article (https://doi.org/10.1007/s11696-020-01236-9) contains supplementary material, which is available to authorized users.

✉ Chinnadurai Anbuselvan
cas_amu@yahoo.co.in

[1] Department of Chemistry, Annamalai University, Annamalainagar, Chidambaram 608 002, India

[2] Present Address: Department of Chemistry, Government Arts College, Chidambaram 608102, India

responsible for their accumulation in the human body, and this occurrence has been coupled to the tumors, insurgence of allergies, and other serious diseases above the genetic pathologies, particularly in children (Lvova et al. 2016). Among the different transition metals, Ni^{2+} ion is an essential nutrient for living organisms incorporating into the biological process lists such as biosynthesis, metabolism, and respiration (Prabhu et al. 2017). The Ni^{2+} ion, in particular at big doses, results in genotoxic and also mutagenic activity, and its genotoxicity might be aggravated by the generation of DNA-damaged ROS (reactive oxygen species) and inhibited of DNA (deoxyribonucleic acid) repairs (Inoue et al. 1997). The small amount of Ni^{2+} examined is very often investigated through diverse methods such as inductively coupled plasma-mass spectroscopy (Fujishiro et al. 1994) and atomic absorption spectroscopy (Miller et al. 2001; Lidén et al. 2008). Among different metal ions over Fe^{3+} ions being a vital element with the human body, it plays a much important role factor in the growth and improvement of living systems (Madhu and Sivakumar 2019a, b). Recent research shows that the Fe^{3+} participates in a few neurodegenerative diseases both of Parkinson's and Alzheimer's disease (Madhu and Sivakumar 2019a, b). And, either it is a deficiency or an excess in the body which had generally persuaded several disorders with iron smuggling and storage, and the balance being tightly uncomfortable in an organism (Zhang et al. 2018). Provided the paramagnetic nature of Fe^{3+}, fluorescent chemosensors were based on the fluorescence quenching mechanism (Wu et al. 2018). And also the most important is to maintain the redox balance of labile iron species which can generate iron catalysis reaction of oxygen species (ROS) (D'Autréaux et al. 2005; Galaris et al. 2008; Natarajan et al. 2019). Between inadequacy and excess of iron absorption in the human body cause cellular homeostasis and also cause different biological diseases (Haas and Brownlie 2001; Thum and Anker 2007; Zheng et al. 2005; Bonda et al. 2011; Pithadia and Lim 2012). Mg^{2+} ions are among the majority abundant divalent metal cations present in cells and play crucial roles in numerous cellular processes such as the proliferation of cells, stabilization of DNA conformation, and enzyme-driven biochemical reactions (Hariharan and Anthony 2014). A deficient and excessive amount of metal ions leads to several diseases. The main source is drinking water which gives magnesium in fair quantities. The standard technique for the determination of Mg^{2+} ions in drinking water is with EDTA complexometric titration (Li et al. 2016). A drug designed and synthesized as a chemosensor for Mg^{2+} recognition in an aprotic solvent with far above the ground selectivity is desired (Marimuthu and Ramu 2018). Schiff bases are unique classes among discovered and had drawn special attention by tempting to the chemists for their manufacture access, efficient chemical and physical properties, and easy isolation, and, in addition, applications as the synthesis of coordination ligand, catalysis, molecular ion recognition, magnetic properties, and optical properties (Chowdhury et al. 2018) Schiff base compounds are called "privileged compounds" because they are shortly synthesized with the condensation of both aldehydes and amines, a well-known one. The strong ability of Schiff base–metal complexes enables their use across a different range of fields, to catalysis, from medicine, fluorescent sensors, and chemosensors (Abdel-Rahman et al. 2013, 2014, 2016, 2017, 2018 ; Abu-Dief and Nassr 2015, Abdel-Rahman et al. 2019a, b, 2020; Al-Saeedi et al. 2018; Gao et al. 2018). There are different processes answerable for the photophysical reaction of these fluorophores for detection of Ni^{2+}, Fe^{3+} and Mg^{2+} ion, such as photoinduced electron transfer (PET) (Banerjee et al. 2013; Sahana et al. 2013; Zhou et al. 2015), excited-state ESIPT (intramolecular proton transfer) (Dhineshkumar et al. 2018; Qin et al. 2015a, b, c; Hossain et al. 2015; Qin et al. 2015a, b, c), CHEF (chelation-enhanced fluorescence) (Ta et al. 2019; Dhineshkumar et al. 2020), ICT (internal charge transfer) (Dhineshkumar et al. 2019; Maity and Govindaraju 2012), FRET (fluorescence resonance energy transfer) (Qin et al. 2015a, b, c; Kim et al. 2008), and C=N isomerization (Kim et al. 2014). Water pollution is the contamination of bodies of water (such as groundwater, aquifers, rivers, lakes, seas, and oceans) typically caused by human activities. Water pollution is any change in water's physical, biological, or chemical properties that would be harmful to any living organism (Ali et al. 2005, 2013, 2016, 2017, 2018; Alharbi et al. 2018). Drinking water, also known as potable water, is the water considered safeenough for both animal and human use. This is water, usually used to wash, drink, eat, irrigate crops, etc. Chemicals, bacteria, and other pollutants affect even our drinking water these days (Basheer 2018a, b; Basheer and Ali 2018; Burakova et al. 2018).

In the part of this research, a Schiff base chemosensor has been synthesized and characterized by $^{1}H\&^{13}C$-NMR, FT-IR, and ESI–MS spectroscopy. The chemosensor is studied by UV–visible and fluorescence measurement and found to recognize three metal ions such as Ni^{2+}, Fe^{3+}, and Mg^{2+} using 10 mM HEPES buffer in EtOH/H_2O (1:4, *v*/*v*, pH = 7.0) medium. Competitive metal ion studies and associated constant value are also predicted. In chemosensor sensing achieved by PET mechanism due to linked nitrogen atom by forming the metal complex, it is followed by a 1:1 ratio of stoichiometry.

Experimental

Chemicals and reagents

The essential materials used were high purity of Analar grade indole-3-carbaldehyde and substituted aldehydes purchased from (India) Sigma–Aldrich and used without further purification. To prepare the solutions of different metal ions, the nitrate or chlorate salts of Cu^{2+}, Fe^{3+}, Mg^{2+}, Mn^{2+}, Ni^{2+}, Zn^{2+}, Pb^{2+}, Cd^{2+}, Al^{3+}, Hg^{2+}, Ca^{2+}, Sn^{2+}, Sr^{2+}, V^{3+}, and Ti^{3+} were used in distilled water for this experiment. The compounds were confirmed and investigated by ^{1}H &^{13}C-NMR, FT-IR, and ESI–MS spectroscopy. Interestingly, the ^{1}H NMR spectrum was recorded on a Bruker-400 MHz and ^{13}C NMR 100 MHz enhancement of the employed with TMS as an internal standard in DMSO-d_6, respectively. Infrared measurement was calculated at 4000–400 cm^{-1} region on an Agilent Carry 630 FT-IR spectrometer. UV and fluorescence measurements were conducted on a PerkinElmer LS45 fluorescence spectrophotometer with a scan rate at 1200 nm at room temperature. For fluorescence measurements, the emission and excitation are at distanced enhancement value, respectively.

Synthesis of the chemosensor ICPA

(4)-4-(phenyldiazenyl)aniline (0.34 g, 1 mmol) and indole-3-carbaldehyde (0.29 g, 1 mmol) were added with 20 mL absolute CH_3CH_2OH in a RB (round-bottom) flask and refluxed for 12 h. The solution was continuously cooled at room temperature and added with absolute distill water to form a yellow precipitate solution. The solution was filtered and washed with H_2O and then recrystallized from ethanol. As shown in Scheme 1 Yield: 0.5 g, 55%. M.p = 197 °C; FT-IR (KBr, cm^{-1}): 3429 (νN–H), 2979 (νAr–C–H), 2927 (νAli.C–H), 1628, 1605 (νC=N), 1576, 1503, 1438 (νC=C), 1389–1194 (βC–H), 1120 (βN–H), 1082–691 (ΓC–H) shown in Fig S1; 400 MHz DMSO-d_6 (^{1}H NMR) 9.9 (*s*, NH), 8.31–8.28 (*t*, 3H *J* = 1.2), 8.09–8.07 (*d*, 2H *J* = 7.6), 7.954–7.932 (*d*, 2H *J* = 8.8), 7.70 (*s*. 1H), 7.52–7.50 (*d*, 2H *J* = 8.0), 7.28–7.21 (7H *J* = 2.6), 7.73 (*s*, –ArH), 6.60–6.58 (*d*, –ArH *J* = 8.8) shown in Fig S2; 100 MHz, DMSO-d_6, (^{13}C NMR) ppm: 155.66, 153.91, 149.18, 138.43, 136.99, 135.57, 128.33, 126.36, 125.42, 124.06, 123.42, 122.09, 120.77, 118.11, 112.37, 112.33 shown in Fig S3: Anal. Calcd for $C_{13}H_{16}N_4$: 365.00 shown in Fig S4.

UV–visible and fluorescence titration measurements

In this experiment, chemosensor **ICPA** (0.0032 mg, 0.001) was dissolved in absolute ethanol (10 mL) and different metal ions such as Fe^{3+}, Co^{2+}, Ni^{2+}, Cu^{2+}, Pb^{2+}, Mn^{2+}, Cd^{2+}, Zn^{2+}, Al^{3+}, Hg^{2+}, Sn^{2+}, Ca^{2+}, V^{3+} Sr^{2+}, and Ti^{3+} (50 µM) were also dissolved in absolute distil water. The stock solutions were diluted with 10 mM HEPES buffer (pH = 7.0) to make the final concentration (50 µM). A variety of stock solutions (0.5 equiv) with the solution of metal ions including 0.5 equiv were makeup in CH_3CH_2OH/H_2O (1:4, *v*/*v*, pH = 7.0). Fluorescence and UV–Vis spectra were taken at room temperature.

Job's plot studies

The stock solutions of **ICPA** (0.0036 mg, 0.002 mmol) were diluted with 10 mM HEPES buffer in $EtOH/H_2O$ (1:4, *v*/*v*) medium to make a concluding concentration of 5.0, 4.5, 4.0, 3.5, 3.0, 2.5, 2.0, 1.5, 1.0, and 0.5 µM and transferred to quartz cells. For metal solutions, 0.5 µM of the Ni^{2+}, Fe^{3+}, and Mg^{2+} solution (10 mM) were diluted to 10 mM HEPES buffer in $EtOH/H_2O$ (1:4, *v*/*v*) medium with 0.5, 1.0, 1.5, 2.0, 2.5, 3.0, 3.5, 4.0, 4.5, and 5.0 µM with ICPA and fluorescence spectra were taken at room temperature.

Cell culture and cytotoxicity assays

HeLa cells were grown in DMEM (Dulbecco's modified Eagle's medium) supplemented with 10% FBS. All cells were supplemented with an (0.1 mg mL^{-1} streptomycin, 0.25 mg mL^{-1} amphotericin B and 100 units mL penicillin) antibiotic antimycotic solution and grown-up at 37 °C in standard (5% CO_2, 95% humidity) cell culture conditions. HeLa cells were cultured in culture media (DMEMC, High Glucose) in an atmosphere of 95% air and 5% CO_2 at 37 °C. The cells were seeded into 96-well plates at a density of 4×10^3 cells per well in culture media, and then (1) 0, (2) 7.8, (3) 15.6, (4) 31.2, (5) 62.5, (6) 125, (7) 250, (8) 500, (9) 1000, and (10) 2000 µM (final concentration) compounds were added. The cells were an atmosphere of 95% air and 5% CO_2 for 24 h then incubated at 37 °C. The absorbance of the cells was measured by ELISA.

Scheme 1 Synthesis of compound **ICPA**

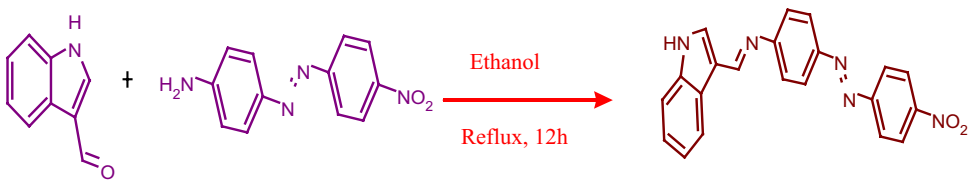

Results and discussion

The chemosensor's response is often described by spectroscopic methods (Fluorescence and UV–Vis spectroscopy) with various cations such as detectable silent substances. The chemosensor **ICPA** shows that it is sensitive to certain metal cations. Addition of 1.0 equiv. of Cu^{2+}, Mn^{2+}, Ni^{2+}, Fe^{3+}, Co^{2+}, Zn^{2+}, Pb^{2+}, Hg^{2+}, Al^{3+}, Cd^{2+}, Ca^{2+}, Sn^{2+}, Sr^{2+}, V^{3+}, and Ti^{3+} cations into the **ICPA** leads to the change of absorption and fluorescence spectra.

UV–visible studies

Absorption spectrum behavior of chemosensor **ICPA** (10 μM) was investigated in EtOH/H_2O medium (1:4, *v*/*v*, and pH 7.0 and 10 mM buffer solution HEPES) at room temperature. The selectivity of different heavy metal ions such as Ni^{2+}, Fe^{3+}, Co^{2+}, Zn^{2+}, Cu^{2+}, Pb^{2+}, Hg^{2+}, Al^{3+}, Ca^{2+}, Cd^{2+}, Sn^{2+}, Sr^{2+}, Mn^{2+}, V^{3+}, and Ti^{3+} (50 μM) was carried out by spectroscopic studies as shown in Fig. 1a.

When added 0.5 equiv concentration of chemosensor **ICPA** in various metal ion (0.5 equiv) concentrations'

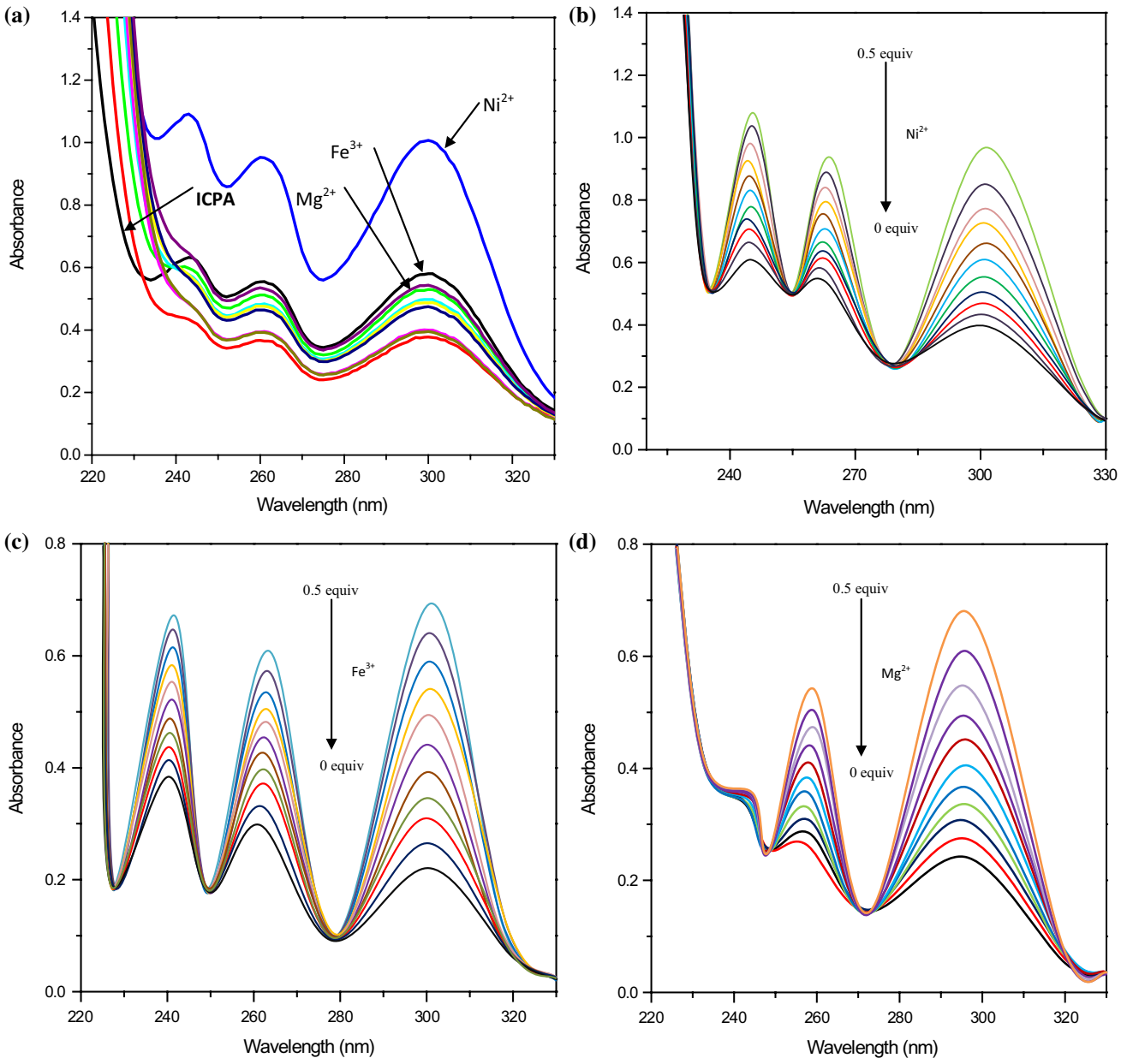

Fig. 1 **a** Absorption spectrum of ICPA (10 μM) with 0.5 equiv of various metal ions used in EtOH/H_2O (1:4, *v*/*v*, pH 7.0) 10 mM HEPES buffer solution, **b** upon addition of Ni^{2+}, **c** upon addition of Fe^{3+}, **d** upon addition of Mg^{2+}

absorption of three bands at 243, 260, and 299 nm appeared, while the mentioned peaks are for Ni^{2+} ion, also for the all transition metal ions. Chemosensor **ICPA** responsibility for another two metal ions Fe^{3+} and Mg^{2+} shows a slight increase from other metal ions, as two absorption band peaks at 260 nm and 299 nm appeared while initial absorption peak at 243 nm disappears. However, 0.5 equiv of Ni^{2+} ion addition increases gradually the binding of chemosensor **ICPA** to provide the three absorption bands one at 243 nm, while new absorption band peaks at 260 and 299 nm normally decreased with concentration (Fig. 1b). Both binding formations of Fe^{3+} and Mg^{2+} (0.5 equiv) used with chemosensors **ICPA** show the first absorption band at 260 nm slightly decrease while concomitantly at 299 nm decreased (Fig. 1c and d).

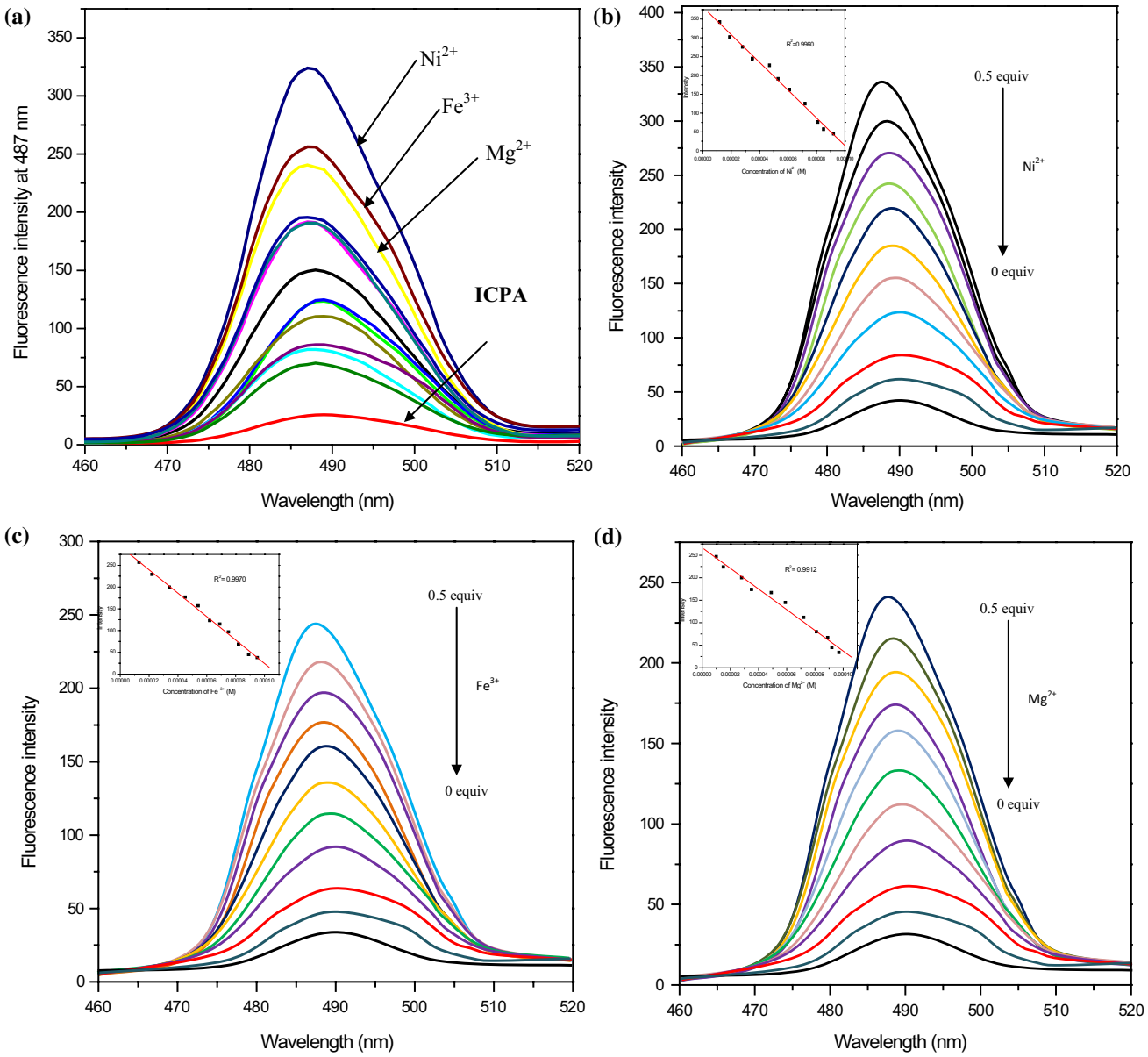

Fig. 2 **a** Fluorescence spectra of **ICPA** (20 μM) in the presence 0.5 equiv of various metal ions in EtOH/H_2O (1:4, *v*/*v*, pH 7.0) 10 mM HEPES buffer solution (λex = 299 nm). **b** Fluorescence titration spectra of receptor **ICPA** (10 μM) used in EtOH/H_2O (1:4, *v*/*v*, pH 7.0) 10 mM HEPES buffer solution upon incremental addition of Ni^{2+} (0–5.0 equiv.). **c** Fluorescence titration spectra of receptor **ICPA** (20 μM) in EtOH/H_2O (1:4, *v*/*v*, pH 7.0) 10 mM HEPES buffer solution upon incremental addition of Fe^{3+} (0–2.4 equiv.). **d** Fluorescence titration spectra of receptor **ICPA** (20 μM) in EtOH/H_2O (1:4, *v*/*v*, pH 7.0) 10 mM HEPES buffer solution upon incremental addition of Mg^{2+} (0–2.4 equiv.). Inset: (λex = 299 nm, λem = 487 nm)

Fluorescence studies

Fluorescence studies for chemosensor **ICPA** (20 μM) participated with different heavy metal ions such as Ni^{2+}, Fe^{3+}, Co^{2+}, Pb^{2+}, Cu^{2+}, Mn^{2+}, Cd^{2+}, Hg^{2+}, Al^{3+}, Ca^{2+}, Zn^{2+}, Sn^{2+}, Sr^{2+}, V^{3+}, and Ti^{3+} (50 μM) carried out in EtOH/H_2O medium(1:4, *v*/*v*, and pH 7.0 and 10 mM HEPES buffer solution) at room temperature. Upon 0.5 equiv addition of different metal ions react with 0.5 equiv of chemosensor **ICPA**, the fluorescence intensity around at 487 nm appeared while excitation wavelength at 299 nm as shown in Fig. 2a. Therefore, fluorescence "turn-on" for selectively of three metal ions Ni^{2+}, Fe^{3+}, and Mg^{2+}, which lead to a slight decrease or increase to all other the transition heavy metal ions. The chemosensor **ICPA** is completely involved downfield below all metal ions. The presence of three metal ions Ni^{2+}, Fe^{3+}, and Mg^{2+} could be displayed in "Off–On" fluorescence behavior on the spectroscopic measurement experiment. Also the sensing of chemosensor **ICPA** behavior in different concentrations in EtOH/H_2O medium (1:4, *v*/*v*, pH 7.0) is provided by Ni^{2+}, Fe^{3+}, and Mg^{2+}. Upon the addition of Ni^{2+} (0.5 equiv) increase, the (fluorescence) intensity at 487 gradually increased in Fig. 2b, and it was great that the linear relationship of emission intensity at 487 nm in that concentration Ni^{2+} (0–5.0 equiv) ($R^2 = 0.9960$) could be seen in Fig. 2b. The intensity was evaluated through the limit of detection calculated at 6.82×10^{-7}M. Furthermore,

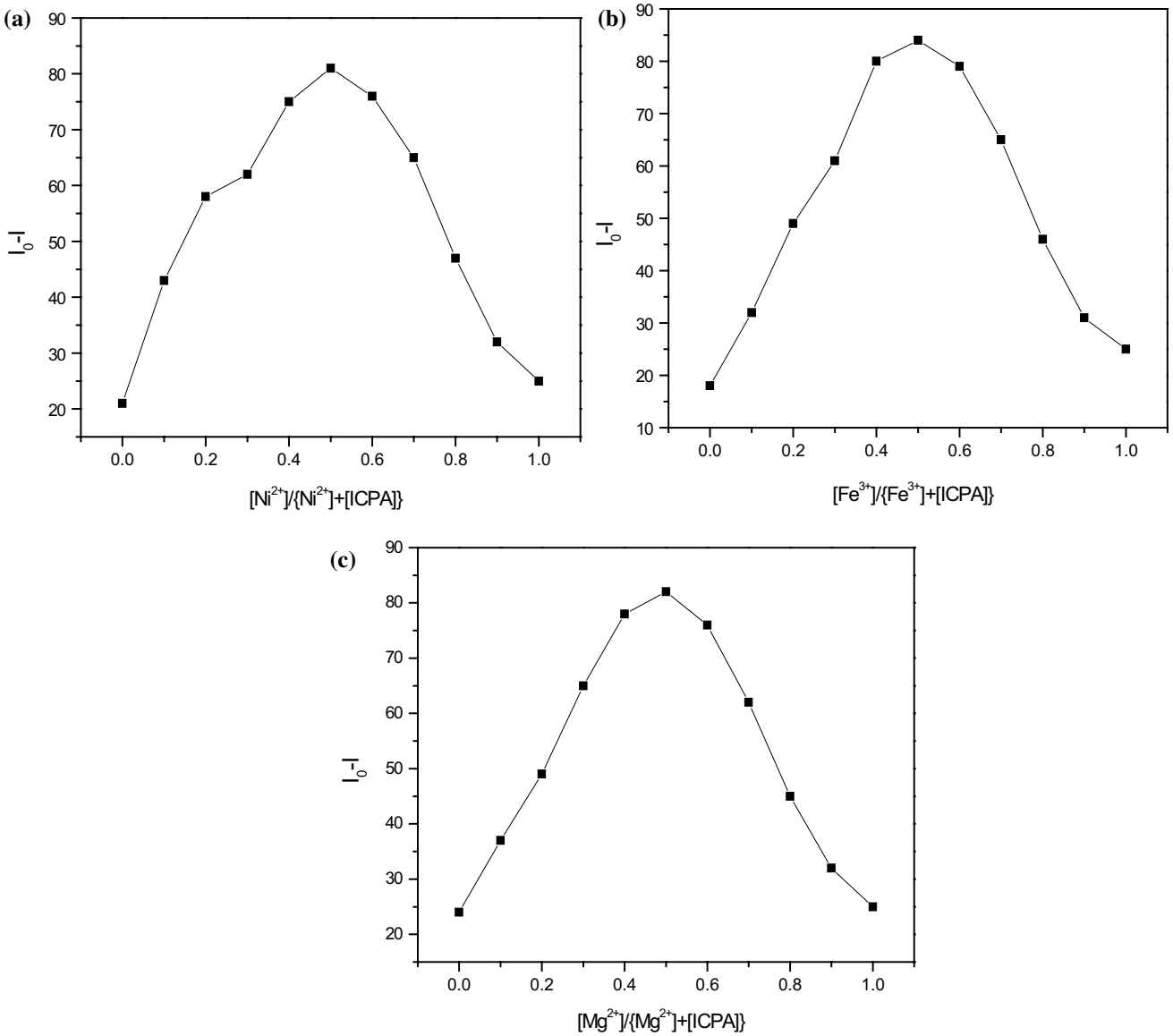

Fig. 3 Job's plot of the **ICPA**-Ni^{2+} complexes in EtOH/H_2O (1:4, *v*/*v*, pH 7.0) 10 mM HEPES buffer solution, keeping the total concentration of **ICPA** (20 μM) and **a** Ni^{2+}, **b** Fe^{3+}, and **c** Mg^{2+} (0–5.0 equiv.) indicating 1:1 stoichiometry at intensity = 487 nm

with the gradual increase in Fe^{3+} (0.5 equiv), the 487 nm fluorescence intensity gradually increased in Fig. 2c.

The good linear relationship of the emission intensity at 487 nm predicted with the concentration of Fe^{3+} (0–20 μM) ($R^2 = 0.9970$) could be seen (inset in Fig. 2c), and the result was evaluated by the limit of detection 5.27×10^{-7} M. Finally, with 0.5 equiv of Mg^{2+} ions gradually increasing with the fluorescence intensity at 487 nm (Fig. 2d), a linear relationship was assumed that the fluorescence intensity with different concentrations of selectivity for Mg^{2+} (0–20 μM) ($R^2 = 0.9912$) could be seen (inset in Fig. 2d, with the detection limit calculated 5.96×10^{-7}M. Chemosensor **ICPA** binding affinity with the selectivity of Ni^{2+}, Fe^{3+}, and Mg^{2+} was examined by fluorescence experiments. A Job plot indicated that 1:1 stoichiometric complex of **ICPA** + Ni^{2+}, **ICPA** + Fe^{3+}, and **ICPA** + Mg^{2+} has been predicted different concentrations by each 0.5 equiv of Ni^{2+}, Fe^{3+}, and Mg^{2+}.

These results confirmed by Job's plot with 1:1 stoichiometric complexes with chemosensor **ICPA** were detected to maximum at 0.5 μM mole fraction determined through the binding addition of $[Ni^{2+}]/\{[Ni^{2+}] + [\mathbf{ICPA}]\}$, $[Fe^{3+}]/\{[Fe^{3+}] + [\mathbf{ICPA}]\}$ and $[Mg^{2+}]/\{[Mg^{2+}] + [\mathbf{ICPA}]\}$, respectively (Fig. 3a–c). In combination with fluorescence titration in EtOH/H_2O (1:4, *v*/*v*, pH 7.0) 20 mM HEPES buffer solution, the association constants (K_a) for **ICPA** + Ni^{2+}, **ICPA** + Fe^{3+} and **ICPA** + Mg^{2+} have been determined by Benesi–Hildebrand method and calculated as 3.45×10^8 M^{-2} (Fig. 4a), 5.63×10^4 M^{-2} (Fig. 4b) and 8.63×10^3 M^{-2} (Fig. 4c), respectively.

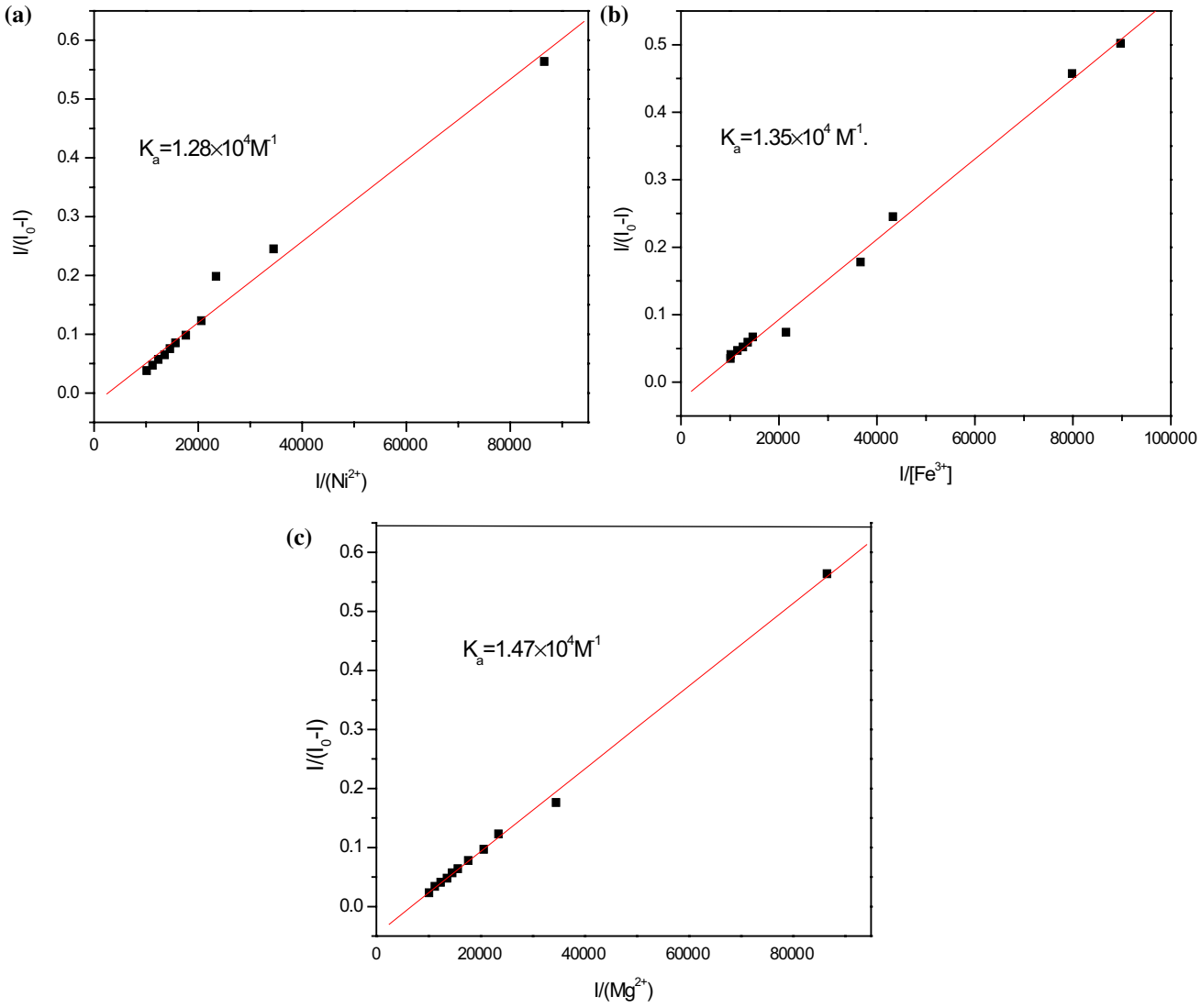

Fig. 4 **a** Benesi–Hildebrand plot of **ICPA** using 1:1 stoichiometry for the association between **ICPA** and Ni^{2+}. **b** Benesi–Hildebrand plot of **ICPA** using 1:1 stoichiometry for the association between **ICPA** and Fe^{3+}. **c** Benesi–Hildebrand plot of **ICPA** using 1:1 stoichiometry for the association between **ICPA** and Mg^{2+}

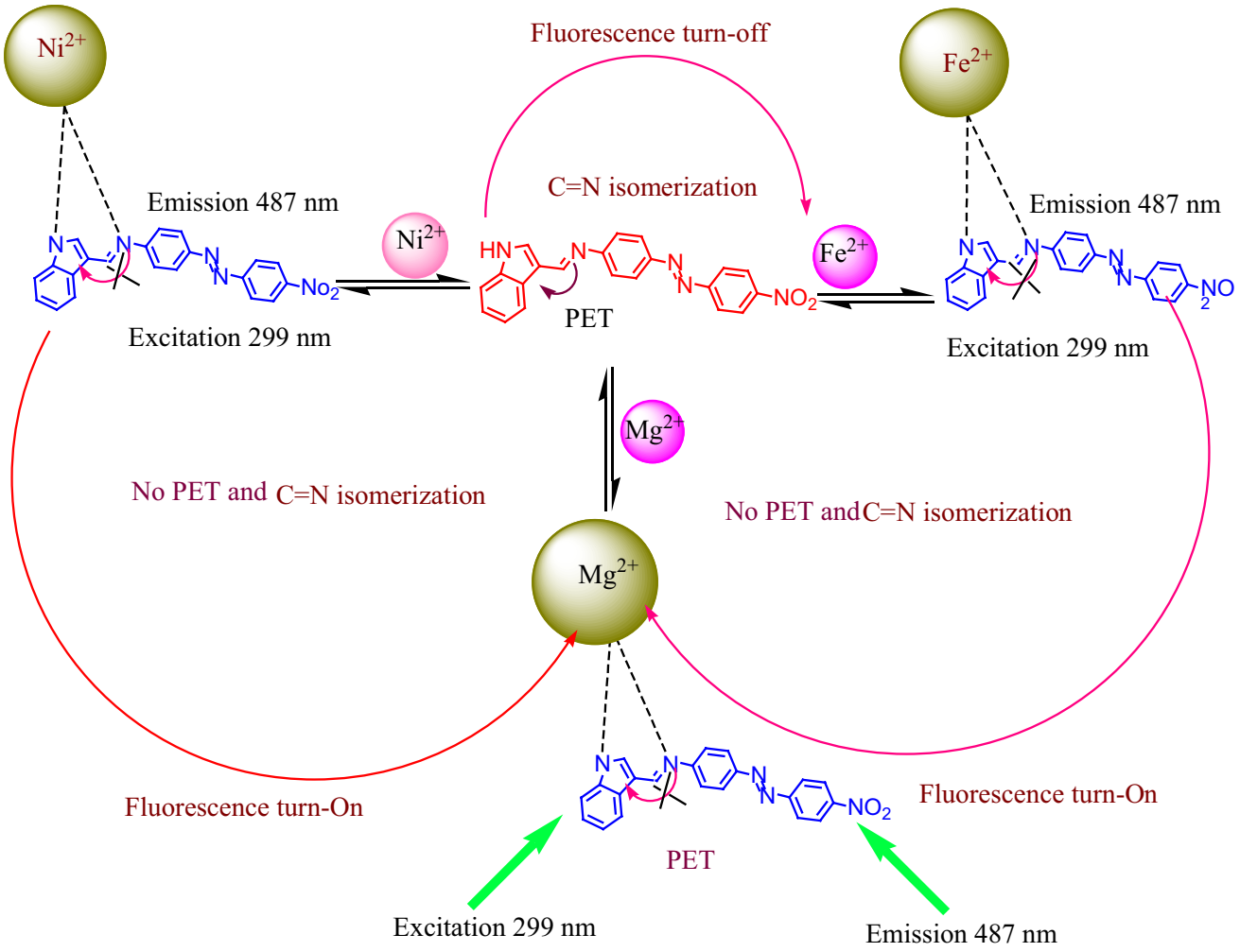

Scheme 2 Proposed binding mechanism of **ICPA**-Ni^{2+}, **ICPA**-Fe^{3+}, and **ICPA**-Mg^{2+}

Proposing the sensing mechanism

The FT-IR spectra recognized the binding mechanism of chemosensor **ICPA**-Ni^{2+} **ICPA**-Fe^{3+} and **ICPA**-Mg^{2+} together analyzed in this experiment (Fig. S5). Chemosensor **ICPA** showed FT-IR peaks at (C=N) group in 1628 cm^{-1} and NH-group in 3429 cm^{-1} obtained. Meantime, 0.5 equiv of Ni^{2+} addition results in the functional group decrease from 1628 cm^{-1} shifted to 1613 cm^{-1} peaks as well as NH-group stretching vibration decrease from 3429 cm^{-1} shifted to 3422 cm^{-1} was obtained (Fig. S5).

Furthermore, 0.5 equiv of Fe^{3+} addition which results in a change from (C=N) 1628 to 1617 cm^{-1}, while NH-group stretching vibration shifted to change from 3429 to 3391 cm^{-1} (Fig. S6). Finally, 0.5 equiv of Mg^{2+} addition with 1628 cm^{-1} shifted to 1620 cm^{-1} gradually decrease peaks observed; however, NH-group stretching vibration shifted to change from 3429 cm^{-1} to 3401 cm^{-1} (Fig. S7). As shown in Scheme 2, the fluorescence "turn-on" in the presence of Ni^{2+}, Fe^{3+}, and Mg^{2+} metal ions, by enhancing emission intensity of the excited state with intersystem crossing to electron and energy transfer mechanism in proposed for chemosensor **ICPA**, emission intensity increases around 487 nm selectively of three metal ions due to inhibition of PET (photoinduced electron transfer) and also >C=N isomerization methods. PET mechanism showed C=N isomerization of imine group "N" to the excited fluorescence indole-dye moiety with more profit of non-radiative decay with excited energy. In Chemosensor **ICPA** (fluorescence turn-on) binding modes with Ni^{2+}, Fe^{3+}, and Mg^{2+} (fluorescence turn-off), these PET and >C=N isomerization method inhibitions caused effective complexation formation.

Competitive metal studies

In this work, the competitive metal ions such as (1×10^6 M^{-1}) Ni^{2+}, Fe^{3+}, Co^{2+}, Hg^{2+}, Al^{3+}, Pb^{2+}, Mn^{2+}, Cd^{2+}, Ca^{2+}, Cu^{2+}, Sn^{2+}, Zn^{2+}, Sr^{2+}, V^{3+}, and Ti^{3+} (50 μM)

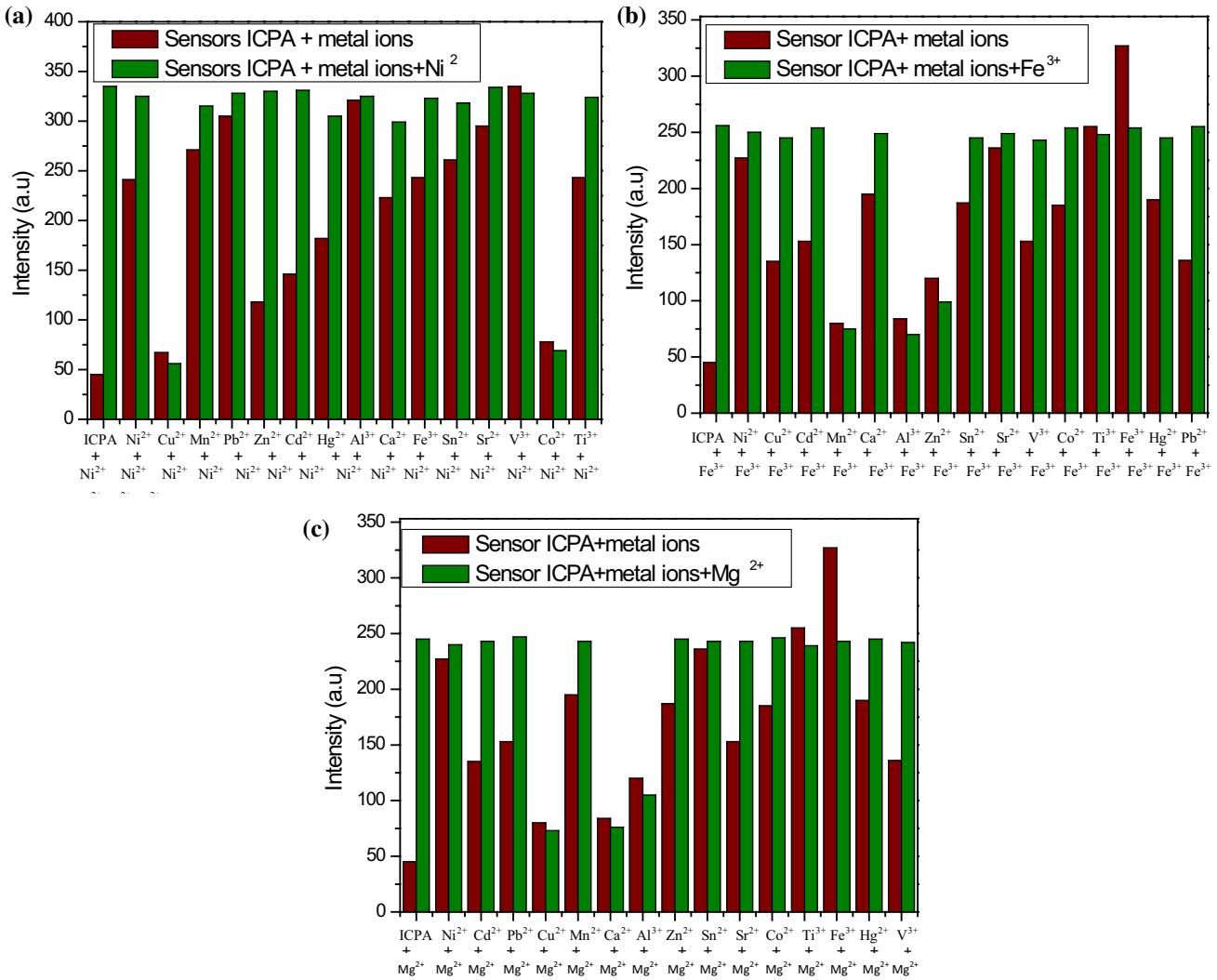

Fig. 5 Fluorescence intensity at 487 nm of **ICPA** (20 μM) upon addition of various metal ions in EtOH/H_2O (1:4, *v*/*v*, pH 7.0) 10 mM HEPES buffer solution. Brown bars represent the fluorescence intensity of **ICPA** in the presence of metal ion (20 μM). Green bars represent the fluorescence intensity in the presence of **a** Ni^{2+}, **b** Fe^{3+}, and **c** Mg^{2+} (50 μM) after the addition of various metal ions

at concentrations mentioned at experimental section were used with the binding of chemosensor **ICPA** (20 μM) and the fluorescence spectra shown in Fig. 3. Addition of 0.5 equiv different metal ions and 0.5 equiv of Ni^{2+} shows an increase in fluorescence intensity at 487 nm while excitation wavelength at 299 nm for Ni^{2+} only. The spectrum revealed that Cu^{2+} and Co^{2+} decreased 100% and 90% by 0.5 equiv of Fe^{3+} ion above the others transition metal ions; therefore, no change for other metal ions due to well-known paramagnetism is shown in Fig. 5a. Similarly, 0.5 equiv of Fe^{3+} with chemosensor **ICPA** binding and 0.5 equiv various metal ions contain best binding interaction with Al^{3+}, Zn^{2+}, and Mn^{2+} gradually decreased from 100%, 90%, and 80% except all metal ions due to which not only paramagnetism, as a result, enormous three metal ions in coordinated 2 + Fe^{3+} compared with highly paramagnetic for **ICPA** +Ni^{2+} as shown in Fig. 5b. Finally, 0.5 equiv of Mg^{2+} concentrating all metal ions contained to bind with chemosensor **ICPA** caused the interaction of transition metal ions Cu^{2+}, Al^{3+} and Ca^{2+} having been decreased level of 100%, 70%, and 50%; consequently, in Cu^{2+} paramagnetic, remaining Al^{3+} and Ca^{2+} are not paramagnetic, while it was great coordinated both sides binding of **ICPA** +Ni^{2+} complexes formation as shown in Fig. 5c. Competitive metal ions completely involved or participated in surroundings.

Reversibility test

This experiment proved that Schiff base chemosensor has been confirmed for practical application with reversibility. The studies of the reversibility experiment of **ICPA** with Ni^{2+}, Fe^{3+}, and Mg^{2+} were carried out compared with

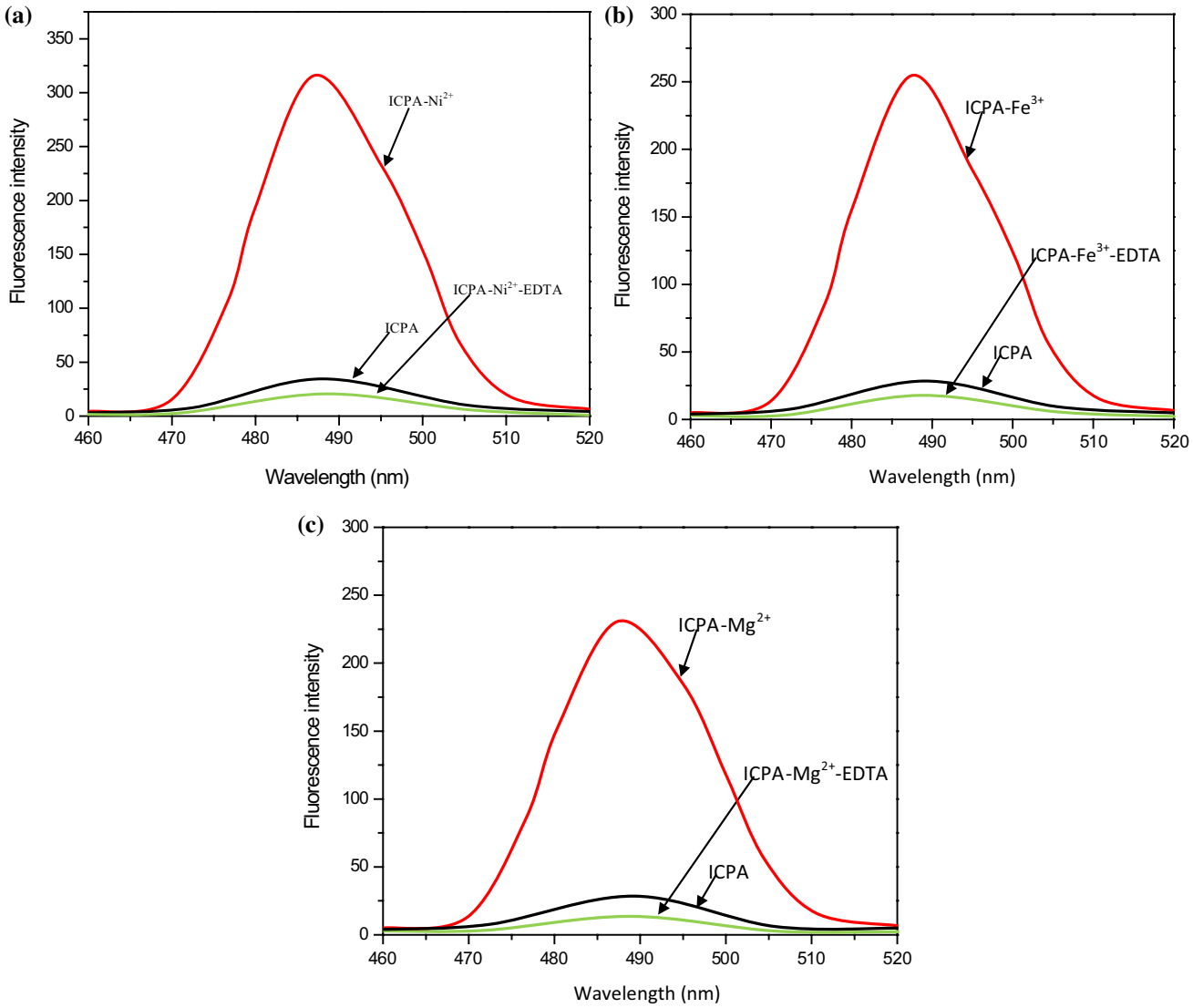

Fig. 6 Fluorescence spectrum of **ICPA** (20 μM) with compared EDTA solution in the presence of **a** Ni^{2+}, **b** Fe^{3+} and **c** Mg^{2+} used in EtOH/H_2O (1:4, *v*/*v*, pH 7.0) 10 mM HEPES buffer solution

EDTA solution. The addition of EDTA solution to **ICPA**-Ni^{2+} complex resulted in the complete quenching its fluorescence intensity; however, **ICPA** solution just showed over EDTA solution; afterward, the solution of **ICPA**-Ni^{2+} complex increases the original fluorescence intensity again; and therefore, result was chemosensor **ICPA** completely reversible sensing for Ni^{2+}as shown in Fig. 6a. Simultaneously, another **ICPA**-Fe^{3+} and **ICPA** + Mg^{2+} complex must be recognized by the same fluorescence intensity at 487 nm between up (Fe^{3+}) and down (Mg^{2+}) as a result of reversible chemosensor, although EDTA solution of both **ICPA**-Fe^{3+} and **ICPA** + Mg^{2+} complexes it is completely quenching fluorescence intensity as shown in Fig. 6b and **c**. These synthesized chemosensors have been compared with the EDTA compound with this experiment.

The cytotoxicity effects

Cancer is a disease caused by an abnormal cell growth that leads to disturbance to other parts of the body, and it is now one of the most dangerous health issues. The combined number of deaths from AIDS, malaria, and tuberculosis is far smaller than those who die from cancer (Rain 2009; Reinberg 2008). The anticancer drugs available on the market have suffered from certain limitations, so the development of new drugs is essential for society (Singh et al. 2009). The indole and its analogs demonstrated a wide spectrum of anticancer activity. We synthesized 4E,10E-4-(2-(4-nitrophenyl)-*N*-((1H-indol-3-yl)methylene)benzenamine and investigated their anticancer activity across the human cancer cell line of HeLa. The cytotoxicity activity of probe

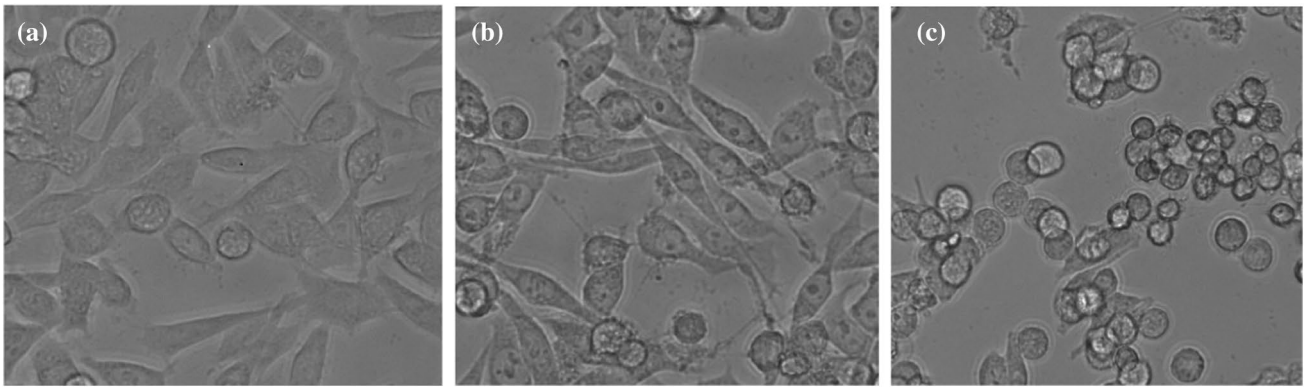

Fig. 7 HeLa cells treatment with ligand **ICPA** in different concentrations **a** empty cell lines, **b** ligand added with cell lines inhibited for a long time, **c** ligand added with whole-cell line killed

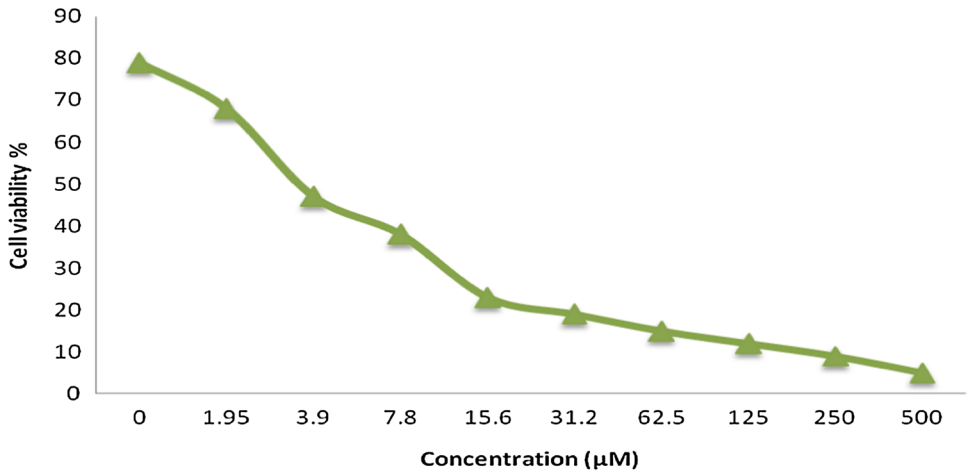

Fig. 8 The cells viability of HeLa cells different concentrations used with ligand **ICPA**

ligand was investigated in different cell lines. HeLa cell lines grown at 37 °C by the culture of different concentrations were prepared in an atmosphere of CO_2-5% and air-95% for 24 h. Furthermore, the Hela cell lines were applied in different concentrations of ligand and have been treated for many hours; it caused much time to kill cancer cells by ligand as exposed in Fig. 7a, in which the first empty plate of HeLa cells before the addition of ligand, the second plate is applied with ligand and cell lines for the time needed to cell death for half of the concentration shown in Fig. 7b.

Finally, the third plate shows the spread of ligand and cancer cells where the complete death of cancer cells within 2 h is exposed in Fig. 7c. The cell viability with an increased order of concentration with the ligand was calculated and detected at 4.7 µM as shown in Fig. 8. As well as, the IC_{50} value also established at different concentrations of ligand shows decreased value due to applied various concentrations of cancer cell lines such as (1) 0, (2) 0.9, (3) 1.95, (4) 3.9, (5) 7.8, (6) 15.6, (7) 31.2, (8) 62.5, (9) 125, (10) 250, and (11) 500 µM in Table 1.

Table 1 IC_{50} values calculated different concentrations of HeLa cells

Hela cells Concentration (µM)	IC_{50} values ICPA
0	100
0.9	79
1.95	68
3.9	47
7.8	38
15.6	23
31.2	19
62.5	15
125	12
250	9
500	5

Conclusion

In this work, we have designed and synthesized a new Schiff base of 4*E*,10*E*-4-(2-(4-nitrophenyl)-*N*-((1H-indol-3-yl)

methylene)benzenamine **ICPA** fluorescent probe which has been evaluated as a sensor for Ni^{2+}, Fe^{3+}, and Mg^{2+} ions by fluorescence "turn-on" response using steady-state absorption and fluorescence spectroscopy. Based on Job's plot, ESI-mass spectral analysis, and Benesi–Hildebrand relation, we propose the structure of ligand and its metal ion as 1:1 stoichiometry complex. This chemosensor exhibits a very good fluorescence sensing ability to Ni^{2+}, Fe^{3+}, and Mg^{2+} ions over are wide pH range. An efficient way for the regeneration of free ligand from the complex probe was achieved using EDTA as a coordinating ligand Ni^{2+}, Fe^{3+}, and Mg^{2+} ions sensing. The MTT assay experiments further demonstrated the cytotoxic in vitro against the HeLa cell line. Thus, the chemosensor meets all the requirements to be an excellent fluorescent probe for wide applications in the field of biolabeling, biosensing, imaging, and so on. Moreover, this work provides a new approach with the economically cheap and less complicated synthetic route for selective, sensitive, and quantitative detection of these three most abundant and essential traces elements in the human body.

Authors' contribution All authors read and sanctioned the final manuscript.

Compliance with ethical standards

Conflict of interest The authors declare that they have no conflict of interest.

References

Abdel-Rahman LH, El-Khatib RM, Nassr LA, Abu-Dief AM, Lashin FED (2013) Design, characterization, teratogenicity testing, antibacterial, antifungal and DNA interaction of few high spin Fe(II) Schiff base amino acid complexes. Spectrochim Acta Part A Mol Biomol Spectrosc 111:266–276

Abdel-Rahman LH, El-Khatib RM, Nassr LA, Abu-Dief AM, Ismael M, Seleem AA (2014) Metal-based pharmacologically active agents: synthesis, structural characterization, molecular modeling, CT-DNA binding studies and in vitro antimicrobial screening of iron (II) bromosalicylidene amino acid chelates. Spectrochim Acta Part A Mol Biomol Spectrosc 117:366–378

Abdel-Rahman LH, Abu-Dief AM, Adam MSS, Hamdan SK (2016) Some new nano-sized mononuclear Cu (II) Schiff base complexes: design, characterization, molecular modeling and catalytic potentials in benzyl alcohol oxidation. Catal Lett 146(8):1373–1396

Abdel-Rahman LH, Abu-Dief AM, Aboelez MO, Abdel-Mawgoud AAH (2017) DNA interaction, antimicrobial, anticancer activities and molecular docking study of some new VO (II), Cr(III), Mn(II) and Ni (II) mononuclear chelates encompassing quaridentate imine ligand. J Photochem Photobiol, B 170:271–285

Abdel-Rahman LH, Adam MSS, Abu-Dief AM, Moustafa H, Basha M, Aboraia AH, Al-Farhan BS, Ahmed HES (2018) Synthesis, theoretical investigations, biocidal screening, DNA binding, in vitro cytotoxicity and molecular docking of novel Cu (II), Pd (II) and Ag (I) complexes of chlorobenzylidene Schiff base: Promising antibiotic and anticancer agents. Appl Organomet Chem 32(12):e4527

Abdel-Rahman LH, Abu-Dief AM, Shehata MR, Atlam FM, Abdel-Mawgoud AAH (2019a) Some new Ag (I), VO (II) and Pd (II) chelates incorporating tridentate imine ligand: design, synthesis, structure elucidation, density functional theory calculations for DNA interaction, antimicrobial and anticancer activities and molecular docking studies. Appl Organomet Chem 33(4):e4699

Abdel-Rahman LH, Abu-Dief AM, Abdel-Mawgoud AAH (2019b) Design, synthesis and structural inspection of some novel di-and tri-azomethene compounds as chemo sensors for the detection of various metal ions. Ann Chem Sci Res 1(4):1–16

Abdel-Rahman LH, Abdelhamid AA, Abu-Dief AM, Shehata MR, Bakheet MA (2020) Facile synthesis, X-Ray structure of new multi-substituted aryl imidazole ligand, biological screening and DNA binding of its Cr(III), Fe(III) and Cu (II) coordination compounds as potential antibiotic and anticancer drugs. J Mol Struct 1200:127034

Abu-Dief AM, Nassr LA (2015) Tailoring, physicochemical characterization, antibacterial and DNA binding mode studies of Cu (II) Schiff bases amino acid bioactive agents incorporating 5-bromo-2-hydroxybenzaldehyde. J Iran Chem Soc 12(6):943–955

Alharbi OM, Khattab RA, Ali I (2018) Health and environmental effects of persistent organic pollutants. J Mol Liq 263:442–453

Ali I, Gupta VK, Aboul-Enein HY (2005) Metal ion speciation and capillary electrophoresis: Application in the new millennium. Electrophoresis 26(21):3988–4002

Ali I, Asim M, Khan TA (2013) Arsenite removal from water by electro-coagulation on zinc–zinc and copper–copper electrodes. Int J Environ Sci Technol 10(2):377–384

Ali I, Al-Othman ZA, Al-Warthan A (2016) Removal of secbumeton herbicide from water on composite nanoadsorbent. Desalin Water Treat 57(22):10409–10421

Ali I, Alothman ZA, Alwarthan A (2017) Supra molecular mechanism of the removal of 17-β-estradiol endocrine disturbing pollutant from water on functionalized iron nano particles. J Mol Liq 241:123–129

Ali I, Alharbi OM, Alothman ZA, Badjah AY, Alwarthan A (2018) Artificial neural network modelling of amido black dye sorption on iron composite nano material: kinetics and thermodynamics studies. J Mol Liq 250:1–8

Al-Saeedi SI, Abdel-Rahman LH, Abu-Dief AM, Abdel-Fatah SM, Alotaibi TM, Alsalme AM, Nafady A (2018) Catalytic oxidation of benzyl alcohol using nanosized Cu/Ni schiff-base complexes and their metal oxide nanoparticles. Catalysts 8(10):452

Banerjee A, Sahana A, Das S, Lohar S, Sarkar B, Mukhopadhyay SK, Matalobos JS, Das D (2013) An INHIBIT logic gate from a thiophene derivative using iron and zinc ions as the input: tuning the efficiency on moving from naphthalene to anthracene to pyrene for the green luminescent detection of the intracellular iron. Dalton Trans 42(46):16387–16395

Basheer AA (2018a) Chemical chiral pollution: impact on the society and science and need of the regulations in the 21st century. Chirality 30(4):402–406

Basheer AA (2018b) New generation nano-adsorbents for the removal of emerging contaminants in water. J Mol Liq 261:583–593

Basheer AA, Ali I (2018) Stereoselective uptake and degradation of (±)-o, p-DDD pesticide stereomers in water-sediment system. Chirality 30(9):1088–1095

Bonda DJ, Lee HG, Blair JA, Zhu X, Perry G, Smith MA (2011) Role of metal dyshomeostasis in Alzheimer's disease. Metallomics 3(3):267–270

Burakova EA, Dyachkova TP, Rukhov AV, Tugolukov EN, Galunin EV, Tkachev AG, Ali I (2018) Novel and economic method of carbon nanotubes synthesis on a nickel magnesium oxide catalyst using microwave radiation. J Mol Liq 253:340–346

Chowdhury B, Karar M, Paul S, Joshi M, Choudhury AR, Biswas B (2018) Salen type ligand as a selective and sensitive nickel (II) ion chemosensor: a combined investigation with experimental and theoretical modelling. Sens Actuat B: Chem 276:560–566

D'Autréaux B, Tucker NP, Dixon R, Spiro S (2005) A non-haem iron centre in the transcription factor NorR senses nitric oxide. Nature 437(7059):769–772

Dhineshkumar E, Iyappan M, Anbuselvan C (2018) Turn on macrocyclic chemosensor for Al^{3+} ion with facile synthesis and application in live-cell imaging. Spectrochim Acta, Part A 199:209

Dhineshkumar E, Iyappan M, Anbuselvan C (2019) Limiting clutches for "turn-on" and "turn-off" chemosensors of 1,2-bis ((E)-9-anthracenyl)methyleneamino)-9,10-anthraquinone. J Mol Struct 1177:545–557

Dhineshkumar E, Iyappan M, Anbuselvan C (2020) A novel dual chemosensor for selective heavy metal ions Al^{3+}, Cr^{3+} and its applicable cytotoxic activity, HepG2 living cell images and theoretical studies. J Mol Struct 1210:128033

Fujishiro Y, Sato T, Okuwaki A (1994) Homogeneous precipitation of transition metal (Co^{2+}, Fe^{2+}, Ni^{2+} and Zn^{2+}) phosphates under hydrothermal conditions utilizing metal polyaminocarboxylate complex as a precursor. Phosphorus Res Bull 4:1–6

Galaris D, Skiada V, Barbouti A (2008) Redox signaling and cancer: the role of "labile" iron. Cancer Lett 266(1):21–29

Gao Z, Feng H, Wang S, Huang Y, Ren X, Pang L, Hu S (2018) Fluorescence turn-on of salicylaldimine ligands by co-ordination with magnesium and amines. New J Chem 42(23):18513–18516

Haas JD, Brownlie T IV (2001) Iron deficiency and reduced work capacity: a critical review of the research to determine a causal relationship. J Nutr 131(2):676S–690S

Hariharan PS, Anthony SP (2014) Selective fluorescence sensing of Mg^{2+} ions by Schiff base chemosensor: effect of diamine structural rigidity and solvent. RSC Adv 4(78):41565–41571

Hossain SM, Lakma A, Pradhan RN, Chakraborty A, Biswas A, Singh AK (2015) Synthesis and characterization of a novel, ditopic, reversible and highly selective, "Turn-On" fluorescent chemosensor for Al^{3+} ion. RSC Adv 5(78):63338–63344

Hyvönen H, Aksela R (2010) Complexation of 3-hydroxy-2, 2′-iminodisuccinic acid (HIDS) with Mg^{2+}, Ca^{2+}, Mn^{2+}, Fe^{3+}, Fe^{2+}, Co^{2+}, Ni^{2+}, Cu^{2+}, and Zn^{2+} ions in aqueous solution. J Coord Chem 63(12):2013–2025

Inoue MB, Medrano F, Inoue M, Raitsimring A, Fernando Q (1997) A new chelating cyclophane and its complexation with Ni^{2+}, Cu^{2+}, and Zn^{2+}: spectroscopic properties and allosterism via ring contraction. Inorg Chem 36(11):2335–2340

Kim HN, Lee MH, Kim HJ, Kim JS, Yoon J (2008) A new trend in rhodamine-based chemosensors: application of spirolactam ring-opening to sensing ions. Chem Soc Rev 37(8):1465–1472

Kim DH, Im YS, Kim H, Kim C (2014) Solvent-dependent selective fluorescence sensing of Al^{3+} and Zn^{2+} using a single Schiff base. Inorg Chem Commun 45:15–19

Li Y, Wu J, Jin X, Wang J, Han S, Wu W, Xu J, Liu W, Yao X, Tang Y (2014) A bimodal multianalyte simple molecule chemosensor for Mg^{2+}, Zn^{2+}, and Co^{2+}. Dalton Trans 43(4):1881–1887

Li Y, Sun J, Sun SP (2016) Mn^{2+}-mediated homogeneous Fenton-like reaction of Fe(III)-NTA complex for efficient degradation of organic contaminants under neutral conditions. J Hazard Mater 313:193–200

Lidén C, Skare L, Vahter M (2008) Release of nickel from coins and deposition onto skin from coin handling–comparing Euro coins and SEK. Contact Dermat 59(1):31–37

Lvova L, Di Natale C, Paolesse R, Giorgi L, Fusi V, Garau A, Lippolis V (2016) Photographic detection of cadmium (II) and zinc (II) ions. Proc Eng 168:346–350

Madhu P, Sivakumar P (2019a) A novel pyridine-pyrazole based selective "turn-off" fluorescent chemosensor for Fe(III) ions. J Photochem Photobiol, A 371:341–348

Madhu P, Sivakumar P (2019b) Selective and sensitive detection of Fe^{3+} ions using quinoline-based fluorescent chemosensor: experimental and DFT study. J Mol Struct 1193:378–385

Maity D, Govindaraju T (2012) A differentially selective sensor with fluorescence turn-on response to Zn^{2+} and dual-mode ratiometric response to Al^{3+} in aqueous media. Chem Commun 48(7):1039–1041

Marimuthu P, Ramu A (2018) A ratiometric fluorescence chemosensor for Mg^{2+} ion and its live cell imaging. Sens Actuat B: Chem 266:384–391

Miller CR, Biswas P, Leikauf GD (2001) Combustion generated nickel species aerosols: Role of chemical and physical properties on lung injury. Aerosol Sci Technol 35(4):829–839

Natarajan V, Thirumalaivasan N, Wu SP, Sivan V (2019) A far-red to NIR emitting ultra-sensitive probe for the detection of endogenous HOCl in zebrafish and the RAW 264.7 cell line. Org Biomol Chem 17(14):3538–3544

Nayab PS, Shkir M (2017) A dual responsive colorimetric and fluorescent reversible turn-on chemosensor for iron (Fe^{3+}): Computational and spectroscopic investigations. Sens Actuat B: Chem 245:395–405

Pithadia AS, Lim MH (2012) Metal-associated amyloid-β species in Alzheimer's disease. Curr Opin Chem Biol 16(1–2):67–73

Prabhu J, Velmurugan K, Raman A, Duraipandy N, Kiran MS, Easwaramoorthi S, Nandhakumar R (2017) A simple chalcone based ratiometric chemosensor for sensitive and selective detection of Nickel ion and its imaging in live cells. Sens Actuat B: Chem 238:306–317

Qin JC, Yang ZY, Wang GQ (2015a) A novel ratiometric fluorescent probe for detection of Fe^{3+} by rhodamine–quinoline conjugate. J Photochem Photobiol, A 310:122–127

Qin JC, Fan L, Wang BD, Yang ZY, Li TR (2015b) The design of a simple fluorescent chemosensor for Al^{3+}/Zn^{2+} via two different approaches. Anal Methods 7(2):716–722

Qin JC, Fan L, Li TR, Yang ZY (2015c) Recognition of Al^{3+} and Zn^{2+} using a single Schiff-base in aqueous media. Synth Met 199:179–186

Rain S (2009) Info NIAC. International Health Organization, Geneva

Reinberg S (2008) Health day news. World Health Organization, Geneva

Sahana A, Banerjee A, Lohar S, Sarkar B, Mukhopadhyay SK, Das D (2013) Rhodamine-based fluorescent probe for Al^{3+} through time-dependent PET–CHEF–FRET processes and its cell staining application. Inorg Chem 52(7):3627–3633

Singh P, Kaur M, Verma P (2009) Design, synthesis and anticancer activities of hybrids of indole and barbituric acids-identification of highly promising leads. Bioorg Med Chem Lett 19:3054–3058

Sun J, Ye B, Xia G, Wang H (2017) A multi-responsive squaraine-based "turn on" fluorescent chemosensor for highly sensitive detection of Al^{3+}, Zn^{2+} and Cd^{2+} in aqueous media and its biological application. Sens Actua B: Chem 249:386–394

Ta S, Das S, Ghosh M, Banerjee M, Hira SK, Manna PP, Das D (2019) A unique benzimidazole-naphthalene hybrid molecule for independent detection of Zn^{2+} and N^{3-} ions: Experimental and theoretical investigations. Spectrochim Acta Part A Mol Biomol Spectrosc 209:170–185

Thum T, Anker SD (2007) Nutritional iron deficiency in patients with chronic illnesses. The Lancet 370(9603):1906

Vijay N, Wu SP, Velmathi S (2019) Turn on fluorescent chemosensor containing rhodamine B fluorophore for selective sensing and in vivo fluorescent imaging of Fe^{3+} ions in HeLa cell line and zebrafish. J Photochem Photobiol, A 384:112060

Wu C, Wang CZ, Zhu Q, Zeng X, Redshaw C, Yamato T (2018) Click synthesis of a quinoline-functionalized hexahomotrioxacalix [3] arene: a turn-on fluorescence chemosensor for Fe^{3+}. Sens Actuat B: Chem 254:52–58

Yiran L, Jiang W, Xiaojie J, Jianwei W, Shuai H, Wenyu W, Jun X, Weisheng L, Xiaojun Y, Yu T (2014) A bimodal multianalyte simple molecule chemosensor for Mg^{2+}, Zn^{2+}, and Co^{2+}. Dalton Trans 43:1881–1887

Zhang S, Sun T, Xiao D, Yuan F, Li T, Wang E, Liu H, Niu Q (2018) A dual-responsive colorimetric and fluorescent chemosensor based on diketopyrrolopyrrole derivative for naked-eye detection of Fe^{3+} and its practical application. Spectrochim Acta Part A Mol Biomol Spectrosc 189:594–600

Zheng H, Weiner LM, Bar-Am O, Epsztejn S, Cabantchik ZI, Warshawsky A, Youdim MB, Fridkin M (2005) Design, synthesis, and evaluation of novel bifunctional iron-chelators as potential agents for neuroprotection in Alzheimer's, Parkinson's, and other neurodegenerative diseases. Bioorg Med Chem 13(3):773–783

Zhou D, Sun C, Chen C, Cui X, Li W (2015) Research of a highly selective fluorescent chemosensor for aluminum (III) ions based on photoinduced electron transfer. J Mol Struct 1079:315–320